Component Analysis of the Visible Absorption Spectra of I_2 and Br_2 in Inert Solvents: A Critique of Band Decomposition by Least-Squares Fitting

Richard Ian Gray, Keith M. Luckett, and Joel Tellinghuisen*

Department of Chemistry, Vanderbilt University, Nashville, Tennessee 37235

Received: July 10, 2001; In Final Form: September 6, 2001

The absorption spectra of I_2 and Br_2 dissolved in *n*-heptane and CCl_4 are recorded with high precision in the visible-near-IR spectral range, at temperatures between 15° and 50 °C. The spectra are decomposed into the three contributing transitions ($^1\Pi_u \leftarrow X$, $B0^+_u{}^3\Pi \leftarrow X$, and A $1_u{}^3\Pi \leftarrow X$) through simultaneous least-squares fitting of the *T*-dependent data. The main results of the analysis are as follows. (1) In I_2 the weakest A ← X band is virtually identical in shape and intensity in these solvents and in the gas phase, but with small blue shifts in solution. (2) The ∼20% increased absorption of I_2 in solution appears to be largely attributable to a doubling in the intensity of the weaker of the two main transitions, $^1\Pi_u \leftarrow X$, which is red-shifted in solution. (3) All three transitions in I_2 shift to the red with increasing *T*, with the strongest effect observed for $^1\Pi_u \leftarrow$ X. These differences are not explained by the refraction-index-based relations commonly used to relate gas- and condensed-phase spectra. In the course of this work the method of decomposition analysis by fitting to assumed band shapes has been tested extensively, with the following observations. (1) The much-used 3-parameter Gaussian and log-normal functions do not have enough flexibility to fit single "pure" bands within the experimental precision obtainable from commercial spectrophotometers. (2) The results of such analyses can vary widely with choice of band function. (3) When comparing two such analyses, lower variance is no guarantee of a "truer" resolution. Concerning the labeling of the halogen electronic states involved in the absorption, it is recommended that for consistency the $^1\Pi_u$ state be designated as the C state in all the halogens.

Introduction

The diatomic halogens absorb light in the UV−visible spectral region, as they undergo electronic transitions from the ground states X $^1\Sigma^+$ to the lowest excited $^1\Pi$ and $^3\Pi$ valence states. These transitions were studied for most of the 20th century and are well understood.[1] In low resolution the spectra generally appear as two or more partially resolved bands at $\lambda > 300$ nm. The absorption is dominated by three transitions: (B″/C) $^1\Pi_u \leftarrow X$, $B0^+_u{}^3\Pi \leftarrow X$, and A $1_u{}^3\Pi \leftarrow X$, in order of increasing wavelength, and generally, decreasing intensity.[2] A typical example among the homonuclear halogens is Br_2, illustrated in the potential diagram of Figure 1. The close proximity of the excited valence potentials and their steep slope in the Franck−Condon region for absorption are responsible for the extensive overlap of these transitions in the spectra. The task of assessing the contributions of the several transitions has inspired considerable effort.[5,7−32] For the homonuclear halogens in the gas phase, this problem was largely solved already by the early 1980s.

The picture is much less clear for the spectra of halogens in solution.[13,33−37] We confine our attention here to just "non-reacting" solvents, such as heptane and CCl_4, which do not give rise to charge-transfer complex formation and associated new spectral bands in the visible and near-UV. Even in such "inert" solvents the spectra are significantly altered, being typically 20% stronger and slightly blue-shifted (see Figures 2 and 3). Yet some bands, for example A ← X in I_2, appear to be equally intense in gas and solution phase. The reasons for such behavior are not understood, but they could be related to the difficulty to fully explain Raman spectra in such solvents.[35,36] The quantitative assessment of the component bands of these solution spectra of I_2 and Br_2 is the primary concern of the present paper.

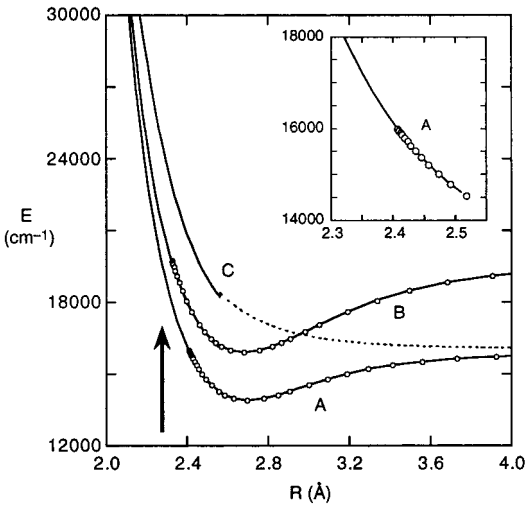

Figure 1. Partial potential diagram for Br_2, showing excited-state potentials involved in the three UV−visible absorption transitions from the ground state. The illustrated points are RKR turning points for the A and B states.[3,4] The repulsive branches of the B and C potentials are from an analysis of temperature-dependent absorption data,[5] while the large *R* region of the C curve (dashed) is from an analysis of spontaneous predissociation of the B state.[6] The small-*R* extension of the A potential (see also inset) is obtained as described in the text. The vertical arrow designates the region of strongest absorption (R_e'') from the X state.

For about half a century, the standard approach for decomposition analysis of low-resolution spectra such as those shown in Figures 2 and 3 has been least-squares (LS) fitting to components of assumed functional form.[38] Gaussian functions

10.1021/jp012618g CCC: $20.00
Published on Web 11/22/2001

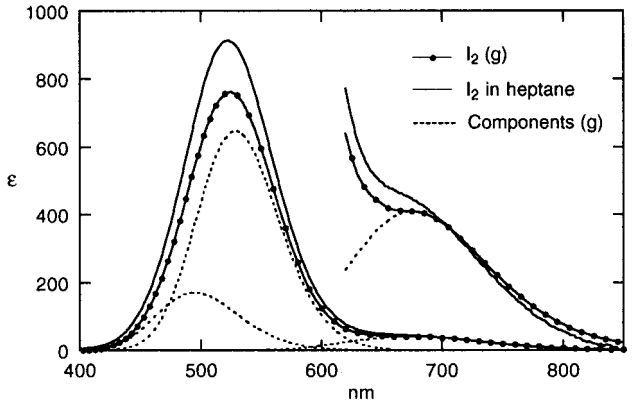

Figure 2. Low-resolution spectra (molar absorptivity, L mol^{-1} cm^{-1}) for I_2(g) and I_2 in *n*-heptane, both at 23 °C. Dashed curves indicate components in the gas phase, from short wavelength to long: C ← X, B ← X, and A ← X.

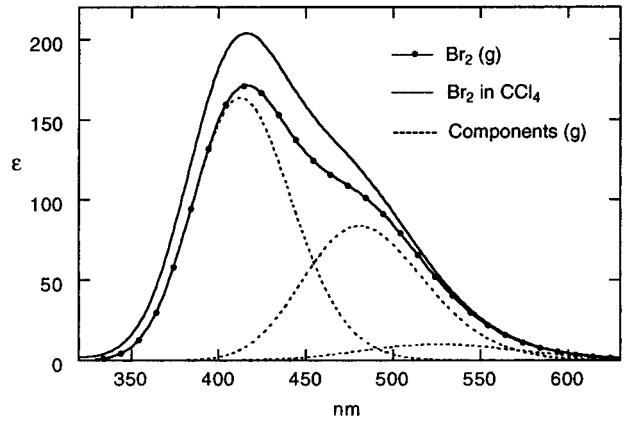

Figure 3. Molar absorptivity of Br_2 in the gas phase and in CCl_4, both at 23 °C. Dashed curves indicate components in the gas phase, ordered as for I_2 in Figure 2.

of the wavenumber ν have probably been the most widely used functions,[7,8,13,34,38] but a number of other forms have been used as well, including especially log-normal functions and variants thereof.[28,29,31,39−41] Yet few workers have taken the trouble to examine the sensitivity of their analyses to the functional forms chosen to represent the components. Where such comparisons have been made, the assumption has been that the statistically best representation of the composite spectrum yields the best component analysis.[28,31,39−42]

However, there is no such guarantee. In fact, as Figure 4 illustrates, just the opposite may be true. Clearly, different inadequate functional forms must yield analyses that are all inadequate to some degree. A measure of that inadequacy (called model error) is the extent to which the fit residuals exceed the experimental error (or equivalently, by how much the reduced chi-square for the fit exceeds 1.0). Some sense of how well the components have been determined can be gained from the spread of results obtained for different assumed component functions. On the latter basis we would have to conclude that the resolutions in Figure 4 have told us little that we did not already know, namely that the spectrum contains (at least) two bands, one stronger than the other.

Even routine spectrophotometric data are so precise these days as to practically ensure that all attempts to decompose a spectrum into 3- or 4-parameter components will prove inadequate at some level of scrutiny.[43] A question of great practical importance then is: When is it "good enough"? The answer to this question will likely differ depending on the primary goal

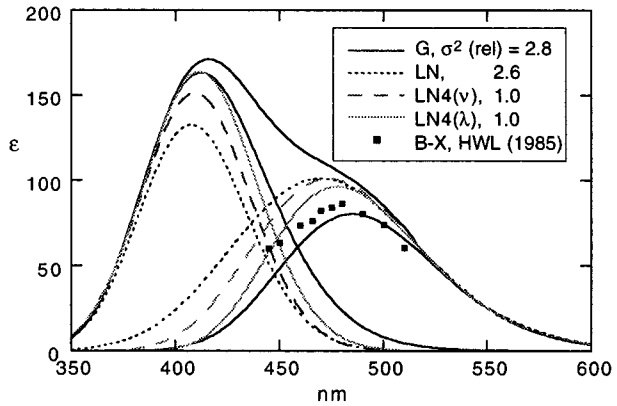

Figure 4. Decomposition analyses of the gas-phase absorption spectrum of Br_2 at 23 °C into two bands, using 3-parameter Gaussian (G) and log-normal functions (LN), and a 4-parameter LN form fitted in both wavelength and wavenumber (details given below). The experimental estimates of B ← X absorption from Haugen et al.[23] (not included in the fits) most closely match the statistically poorest Gaussian analysis.

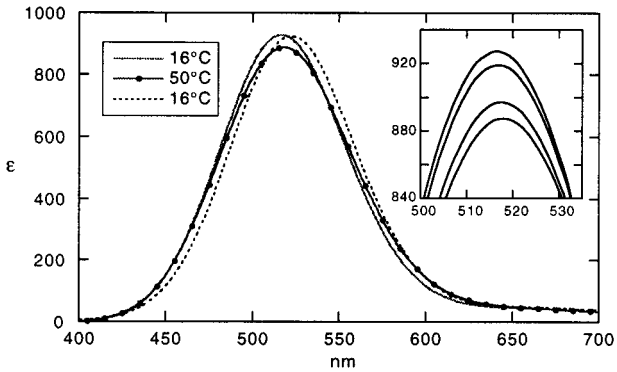

Figure 5. Main peak of the absorption spectrum of I_2 in CCl_4 (solid curves, two temperatures) and in *n*-heptane (16 °C only). The inset is an amplification of the region of the main peak in CCl_4, showing the progressive red shift with increasing T (top to bottom): 15.7 °C, 22.7 °C, 40.2 °C, and 50.0 °C.

of the analysis. Many of the cited examples focused on representing the total spectra compactly through small numbers of parameters. They may well succeed in that goal even while not succeeding in pinning down the true components. (For example, all of the fits in Figure 4 matched the experimental data to within about the thickness of the line.) A preoccupation with this question of adequacy for component analysis has become a second major concern of the present paper. More specifically, when can the LS analysis yield reliable component bands even though it fails the chi-square test?

Related to the latter question is the matter of what kind of additional experimental information might be brought to bear on the problem. For example, the MCD, Raman, and CARS spectra of refs 13, and 35−37 provide information complementary to that contained in the absorption spectra alone and so should aid in the resolution; however, to date it has been difficult to obtain a precise quantitative assessment from such data. In the present study we have used only absorbance data, but recorded over a range of temperatures, with the T dependence representing the only extra "hook" the LS analysis might latch onto in seeking out the true components (see Figure 5). To be sure, temperature dependence has been utilized from the very early days of decomposition analysis.[38] However, the approach taken here is the simultaneous fitting of spectra recorded at multiple temperatures, which, to our knowledge, has not been used previously. A noteworthy exception to this statement is

the comprehensive analysis of the Br_2 gas-phase absorption spectrum carried out by Le Roy, et al.[5] In that work the directly fitted quantities were the potential curves of the B and C states, with the former being well anchored at large internuclear distance R by precise knowledge of the B ← X discrete absorption spectrum (see Figure 1). The same method was used by Burkholder and Bair for Cl_2.[22] One might also choose to fit potential curves instead of spectra for the solution data. However, it is not clear that this would offer any advantage, since the variation of the spectra with solvent makes it clear that the potentials are not the same as for the gas phase and differ somewhat with solvent (Figure 5). Thus the information about the potential wells, which proves so valuable in the gas-phase analysis, cannot be so readily used to advantage in the solution analysis.

In the context of our approach it should now be admitted that the test illustrated in Figure 4 was not completely fair, in that it employed spectra for one temperature only. It also neglected the A← X band (as did Le Roy et al.[5]), which is now fairly well known experimentally.[14,18,24] These defects will be remedied in the work described below, which, however, will still not remove all the ambiguities.

The body of this paper consists of further tests of the assumptions of band decomposition analysis on well-defined gas-phase spectra, followed by application to the solution spectra of I_2 and Br_2. The test computations include application of the Gaussian and log-normal functions and their variants on "exact" (computed) spectra for the individual transitions in I_2, and more proper tests on Br_2(g) of the type illustrated in Figure 4, but with inclusion of the A ← X band. One of the goals of the single-band calculations is to determine how well "real" spectra follow the temperature dependence derived long ago for absorption from a harmonic potential[38] and still incorporated in more elaborate models for the T dependence of low-resolution band spectra.[40]

Before proceeding, we wish to address a problem touched on earlier, namely the matter of inconsistent labeling for the absorbing $^1\Pi_u$ state. It is now well established that this state is the same in all of the homonuclear halogens; it is the $^1\Pi_u$ belonging to the 2431 molecular orbital configuration to which the A and B states also belong.[1] This state has been labeled by Huber and Herzberg[2] as C in Cl_2 and Br_2, but B″ in I_2. Earlier, when the nature of diffuse absorption in the halogens was much less understood, Herzberg used the C label for the 1_u component of a higher $^3\Sigma^+$ state in Br_2 and Cl_2, which dissociates to one ground state ($^2P_{3/2}$) and one excited halogen atom ($^2P_{1/2}$).[44] This state was subsequently identified in I_2 and called C;[45] and that label has persisted.[46] It is clearly desirable to have a common label for this state in the different halogens. In view of its prominent contribution to the valence-state absorption in the homonuclear molecules and its probable similar significance in the heteronuclear species (as the 2431 $^1\Pi$),[23,27,29,32] we believe that it deserves the unprimed C label. Accordingly we have used this designation for both Br_2 and I_2 in the present work. The current C state in I_2 would then have to be relabeled; we suggest C′.

Experiments

All spectra were recorded at a resolution of 1 nm on a Shimadzu UV-2101PC UV−visible spectrophotometer equipped with a temperature-controlled cuvette compartment, at temperatures between 15 °C and 50 °C. The nominal temperature was checked with a calibrated thermistor, resulting in corrections as large as 0.7 °C. The solution spectra were recorded at typically 3−5 different concentrations in a run, spanning an absorbance range of roughly 0.3−1.5. [Absorbance, $A \equiv \log(I_0/I)$, where I_0 and I are incident and transmitted intensity, respectively.] For I_2 this meant concentrations up to 0.0015 mol/L, and about a factor of 5 larger for Br_2. A weighted average of the several spectra was used for the LS fitting; the weights were based on an earlier statistical error calibration of the instrument, obtained by recording spectra of neutral density filters.[47] No check was made of the photometric accuracy, which is stated to be within ±0.004 at $A = 1$ by the manufacturer. The solution concentrations were corrected for T dependence using available density data for the pure solvents: from refs 48−50 for CCl_4 and 48 and 51 for *n*-heptane.

Spectra for gaseous Br_2 were obtained on the same instrument, using a special 1-cm quartz cuvette that was attached to a vacuum line for direct pressure measurement with a quartz bourdon gauge (Texas Instruments). Examination of spectra recorded at different pressures showed no deviations from Beer's law over the wavelength ranges used in the analyses. Similarly, no concentration dependence was observed for the solution spectra.

Spectra of I_2 in *n*-heptane at four temperatures are given in Table 1S (Supporting Information) and of I_2 in CCl_4 in Table 2S. Table 3S gives the spectra of Br_2(g) at two temperatures, and Table 4S covers Br_2 in CCl_4 at four temperatures. For all of these the entered wavelengths (nm) must be corrected in accord with the wavelength calibration reported previously,[43] which includes a sinusoidal wobble of amplitude ~0.05 nm superimposed upon a quadratic function of the fiducial wavelength

$$\Delta\lambda = [0.041 + 0.025 \sin (1.623\lambda - 550)^2] \sin (\pi x/10) + 0.188 + 0.00055\, x + 8.4 \times 10^{-7}\, x^2 \quad (1)$$

All quantities here are in nm, the correction is additive ($\Delta\lambda$ = true − apparent), and the argument $x = (\lambda - \lambda_0)$. The phase λ_0 was "fine-tuned" in the LS fits but was normally close to 637.6 nm.

The statistical errors in the averaged spectra were typically a factor of ~10 larger than would be predicted from the inherent instrumental statistical error. This is as expected if the overall error is dominated by concentration errors for the prepared solutions, and it can result in a false sense of security in the LS fits, because the *shape* of the spectrum is much more precisely defined than is its absolute magnitude. In other words, concentration-based errors are overly pessimistic from the standpoint of band fitting, and they can result in apparent reduced chi-square values much less than 1.0, even for fit models that show clear systematic trends in the fit residuals.[52] The problem of concentration control was considerably greater for Br_2 (in solution) than for I_2, and it included changes with time due to loss from the stoppered (Teflon) cuvettes. This was evidently due to the considerable vapor pressure of Br_2, combined with its large Henry's law constant in CCl_4.[53] For this reason we also extended the Br_2 solution measurements only up to 40 °C. Our absolute absorbances are thought to be reliable to within 1% for I_2, 3% for Br_2; the relative absorbances are a factor of 5 more precise. The peak molar absorptivity (L mol^{-1} cm^{-1}) at 23 °C was 920 for I_2 in both *n*-heptane and CCl_4 and occurred near 523 nm in the former, 517 nm in the latter. For Br_2 in CCl_4 the peak was 200 at 416 nm. (Bromine was not studied in heptane, because the two react in light.)

Compared with the data of Passchier, et al.[8] for gaseous Br_2, our ϵ was slightly larger (171.2) at the peak wavelength of 416,

but still within their quoted error. A larger discrepancy was observed in the 530−560-nm region, with our values lying systematically higher by ∼10%. This is a region of discrete B ← X absorption, where Beer's law can fail, due to saturation within the narrow absorption lines. Under such circumstances, the apparent ϵ will always undershoot the true value, with the latter being observed only in the limit of zero absorption.[11] A check of our spectra at different pressures showed no *P* dependence in ϵ in this region, indicating that our maximum *A* here (0.38) is already sufficiently small to be on the linear growth curve. At our 1-nm resolution, the B ← X vibrational structure is partially resolved, with a maximum amplitude of ∼10% of ϵ around 570 nm. The overall spectrum in this region still varies smoothly with λ, so the effect of this structure should be mainly an artifactual boost in the LS chi-square values.

Although spectra of I_2 in solution have been reported frequently in the literature, we are aware of only one previous study in which precision and temperature dependence were emphasized, that being the work of Geilhaupt and Dorfmüller,[34] who also used *n*-heptane and CCl_4 as solvents. These authors' estimates of peak absorptivity agree with ours within their much larger reported errors (∼7%). Their peak wavelengths at 23 °C agree with ours within ∼1 nm. However, they detected no *T* dependence in the wavelengths of their spectra, in contrast with the behavior observed here and illustrated in Figure 5. On the other hand, we found no significant *T* dependence in the integrated absorptivity, also in agreement with Geilhaupt and Dorfmüller. For example, for the I_2/heptane data in Table 1S, the quantity $\int \epsilon \, d\lambda$ increases with *T* by 0.03% over the experimental *T* range while $\int \epsilon \, d\nu$ decreases 0.4%. The quantity $\int \epsilon \, d \ln\lambda$, which is proportional to the electronic transition strength (see below), decreases by 0.2%.

Theoretical Background

Computed Spectra. For the purpose of the test fitting to single bands, spectra were computed for the three transitions in I_2 using the results of the analysis in ref 21 and standard methods described in ref 54. The C ← X transition is fully diffuse in the spectral region of interest and the A ← X transition is almost so, but the B ← X system is mainly discrete. To generate a suitable low-resolution spectrum for B ← X, we used the pseudo-continuum approach, in which the attractive branch of the potential is removed and the repulsive branch is extended to an artificial lower dissociation limit at large *R*.[54,55] This approach works because for transitions such as this, the Franck−Condon properties are entirely determined by the *shape* of the repulsive branch in the absorption region. The computed spectra included contributions from the lowest 12 v'' levels and were averaged over J'' using five representative rotational values, in the manner of Le Roy, et al.;[5] however, spectra computed for a single J'', taken as the average for the temperature in question, gave very similar results in the fitting tests. The gas-phase spectrum and component bands illustrated in Figure 2 were computed for an assumed temperature of 295 K. Spectra were also computed at 320 K to check on the predicted *T* dependence of the fit models. Note that in the analysis of ref 21, constant transition moment functions were assumed for the C ← X and A ← X transitions, while a transition moment function was derived for B ← X. The same assumptions were used in the present computations, with the B ← X transition moment taken to be a linear function of *R*.

The same computational methods were used to regenerate the C ← X and B ← X component spectra derived (but not tabulated) in ref 5 for Br_2. Again, the B ← X system was made fully diffuse by the pseudo-continuum approach. The RKR potential for the A state of Br_2 is quite well known, practically up to the dissociation limit,[3,56] so it is possible to predict the shape of the A ← X absorption continuum fairly well by smoothly extending the repulsive branch of the A curve to higher energy at small *R*. To obtain such an extension, we examined the B repulsive segment derived by Le Roy et al. and found that with a drop of 2000 cm^{-1} (roughly $T_{e,B} - T_{e,A}$) and a translation to larger *R* by 0.009 Å, the same form nicely matches the left-branch RKR points on the A curve (see Figure 1, inset). This extension yields an A potential that is somewhat steeper than B in the absorption Franck−Condon region (∼2.3 Å) and an A ← X spectrum that is broader on a wavenumber scale. Such a result is reasonable and in line with results for these states in I_2.[21,57] To obtain the A ← X component illustrated in Figure 3, we used this extension and the B ← X transition moment function of Le Roy, et al., and then scaled the spectrum to yield optimal agreement with the experimental data from Hemenway, et al.[18] The resulting computed spectrum is also in good agreement with more recent estimates of the A ← X absorption at shorter wavelengths, from Smedley et al.,[24] even though these authors commented that their values might be too large due to possible contributions from the other two transitions.

Although the A ← X system in Br_2 is weak (maximum ϵ = 10 L mol^{-1} cm^{-1}), its inclusion in the total spectrum does compromise the validity of the Le Roy determination of the other two components. Thus the estimates of these illustrated in Figure 3 were obtained via a least-squares band decomposition fit that included all available experimental data for the A ← X and B ← X bands individually (see below).

Spectral Fitting. Maric and Burrows have provided a comprehensive review of the application of band fitting methods to low-resolution or diffuse diatomic spectra in the gas phase.[40] Most such work has used just 3-parameter band shape functions, like the Gaussian,

$$f_G(x) = a \exp[-b(x - c)^2] \tag{2}$$

and the log-normal,

$$f_{LN}(x) = a \exp[-b(\ln(x/c))^2] \tag{3}$$

The argument *x* can be either wavelength λ or wavenumber ν. Equation 3 is invariant with respect to this choice, but the Gaussian is not, with most spectra fitting better when the argument is taken as ν. Two popular and simple variants on these forms are obtained by multiplying the function by the argument, e.g., $f_{GS}(x) = (x/c)\, f_G(x)$. While this form is reputed to yield physically more meaningful parameters, from a statistical standpoint there is typically negligible difference in fitting to f_G vs f_{GS}. For the log-normal form, Maric, et al.[28] have noted that scaling $f_{LN}(x)$ by the argument still yields the log-normal form, but with the parameters having different significance, i.e., $(x/c)\, f_{LN}(x; a,b,c) = f_{LN}(x; a',b,c')$. Maric and Burrows[40] also suggested 4- and 5-parameter extensions of $f_{LN}(x)$:

$$f_4(x) = \left(\frac{a}{1 - d/x}\right) \exp[-b(\ln(X))^2] \tag{4}$$

$$f_5(x) = \left(\frac{a}{1 - d/x}\right) \exp[-b|\ln(X)|^p] \tag{5}$$

where

$$X \equiv \left(\frac{x - d}{c - d}\right) \tag{6}$$

We have tested all of these forms and, in addition, log-normal functions multiplied by polynomials in $(x - c)$,

$$F_4(x) = f_{LN}(x)\,[1 + d(x - c)^p] \tag{7}$$

$$F_5(x) = f_{LN}(x)\,[1 + d(x - c)^p + g(x - c)^q] \tag{8}$$

In eqs 7 and 8, the parameters p and q are integers set in advance. These two forms have the unfortunate ability to go negative; however, this was never more than a cosmetic problem in our fitting.

Under the simplifying approximations of a harmonic absorbing state, with reflection onto a linear upper potential, the amplitude and width parameters in eq 2 have predictable temperature dependences:[38]

$$a(T) = a_0\,[\tanh(h\omega/2kT)]^{1/2}$$
$$b(T) = b_0 \tanh(h\omega/2kT) \tag{9}$$

where ω is the harmonic frequency and h and k are the usual fundamental constants. In this model there is no T dependence in the location parameter c. Maric and Burrows have provided an approximate physical model for eq 4 and have also derived the T dependence for the parameters in this model.[40] The main results of their derivation are that the T dependences of a and b in eq 4 remain as given in eqs 9, provided that the transition moment function is constant. It follows that the same holds for a and b in the log-normal function of eq 3, since it is just a special form of eq 4. The location parameters c remain independent of T, unless the transition moment function is not constant, in which case eqs 9 are modified, but in a way that typically alters the numerical values of a and b only slightly.

Because the functions given above do not allow for T dependence in the location parameters (except very weakly for eqs 4 and 5), it was necessary to include additional parameters in the fit model to accommodate the different peak positions c at each T in the multispectrum fitting. These functional forms also conserve band area (or nearly so), so if the experimental spectra displayed a significant dependence of total area on T, it was necessary to include parameters to permit deviation from the predicted dependence for the amplitude parameters $a(T)$ given in eq 9. As was noted earlier, there was no significant T dependence in the integrated areas for the I_2 solution spectra. However, there was in some of the Br_2 spectra, both gas phase and solution. In such cases the correction was taken as a single scaling parameter for the entire spectrum at that T, meaning all components were scaled by the same factor. This approach is in keeping with our interpretation that such effects are likely a consequence of experimental limitations.

The width parameters b, on the other hand, were assumed to follow eq 9, meaning that a single parameter b_0 sufficed for each component band at all T. Similarly, the fourth and fifth parameters that occur in eqs 4−8 were assumed to be independent of T. The T dependence is governed by the additional parameter ω (the effective harmonic frequency). The fits never demonstrated very good sensitivity to this parameter, so it was normally fixed at the gas-phase value, which for both Br_2 and I_2 is only a few cm^{-1} larger than the estimated values in these solvents.[58]

On the matter of peak widths, it should be acknowledged that since the experimental spectra were recorded at the bandwidth of 1 nm, the fit model should properly be a convolution of the experimental spectrum with a 1-nm slit function (experimentally Gaussian). This slit width is so small compared with typical component bandwidths (∼100 nm) that one would not expect a sampling model to differ much from a convolution model. Still, to check this we coded a convolution model and compared its results for one I_2/CCl_4 data set. The differences were indeed negligible, the biggest being changes in the b parameters at the part-per-thousand level.

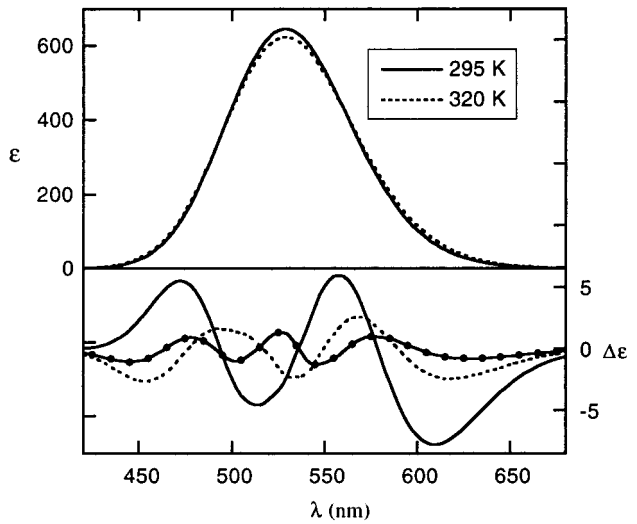

Figure 6. Computed B ← X spectra of I_2(g) at two temperatures, with LS fit residuals (calculated − observed) shown below (scale to right). The solid, dashed, and solid+points curves represent the results from fits of the 295 K spectrum to the 3-, 4-, and 5-parameter log-normal functions of eqs 3−5, respectively.

The least-squares fitting employed standard nonlinear methods.[52] The fits to Gaussian and log-normal basis functions usually converged quickly when initiated with reasonable parameter values. However, convergence was a problem when the 4- and 5-parameter forms of eqs 4 and 5 (and to a lesser extent, eqs 7 and 8) were used, so we devised a Marquardt algorithm[59,60] for handling these band shapes. Interestingly, the 4-parameter function f_4 gave better convergence and lower variance when taken as a function of λ than as a function of ν, even though the approximate physical model behind this form implies $f_4 = f_4(\nu)$.[40]

Results and Discussion

Single Band Fitting. In the tests of eqs 2−8 on single computed transitions in the gas-phase spectrum of I_2, the log-normal form always outperformed $f_G(\upsilon)$ by about a factor of 2, in terms of the summed, squared residuals (SSR). By the same measure, $f_G(\lambda)$ was about a factor of 5 worse than $f_G(\upsilon)$. Not surprisingly, SSR dropped significantly when a fourth and then a fifth parameter were added to the band shape, by typically a factor of 5 in each step. The calculations were done for two weighting assumptions: constant error and uncertainty typical of that for the spectrophotometer used in our experimental work.[47] The results were essentially the same for both assumptions.

Some results of such calculations are illustrated in Figure 6. This display illustrates that for the 3-parameter LN form, the magnitude of the residuals greatly exceeds the typical error in an absorption spectrum obtained from a modern spectrophotometer. This means that model error can be expected to dominate any fit to such a function. Unfortunately, the model error remains significant even for the 4- and 5-parameter forms. For reference, our experimental statistical error translates into

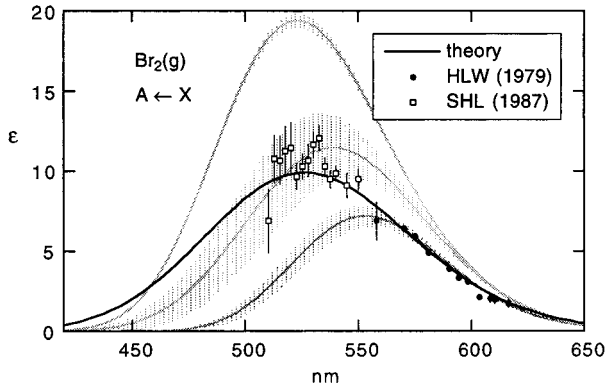

Figure 7. Estimates of the A ← X spectrum of Br_2(g) at 23 °C from decomposition fitting, compared with experimental and theory-based estimates. The experimental points are from refs 18 and 24, while the theory curve was computed from the potentials shown in Figure 1 (see text). The three fitted estimates (shown with 1-σ error bands[61]) were obtained using the scaled Gaussian $f_{GS}(\nu)$ (strongest and weakest) and the log-normal form (middle). For the strongest curve, the peak location parameter was set at a value obtained from the theory-based spectrum.

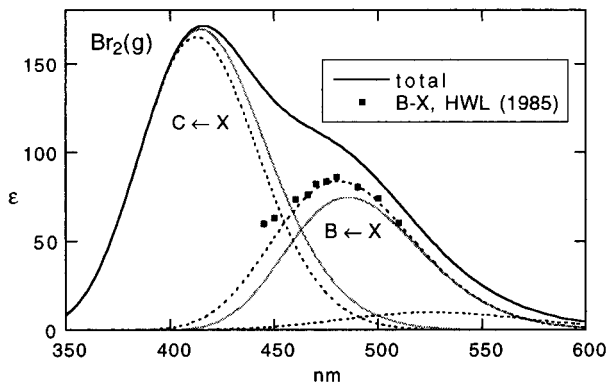

Figure 8. Estimates of the C ← X and B ← X bands of Br_2(g) at 23 °C from decomposition fitting with A ← X held at its theoretical estimate (broad dashed curve at long wavelength). Experimental points are from ref 23. The two components were represented in the 4-parameter form $f_4(\lambda)$ and yielded the dashed curves when the experimental points were included, the shaded curves when they were not. The chi-square was 13% higher for the former fit than for the latter.

$\Delta\epsilon \approx 1$ L mol^{-1} cm^{-1} for a single spectrum recorded under optimum conditions (although instrumental reproducibility roughly doubles this).

To check the T dependence, the spectra at the two temperatures were fitted separately and their parameters compared. (For the 4- and 5- parameter forms, the extra parameters were first fixed at their average values from the two fits.) If the spectroscopic ω_e of I_2(X) (214.6 cm^{-1}) is used in eqs 9, the predicted ratio of the b values is 1.0715 (295 K/320 K). The typical observed values of this ratio ranged from 1.073 to 1.076. While the discrepancy does not seem great, the tanh function is not very sensitive to ω_e and the value 1.073 corresponds to $\omega_e = 200$ cm^{-1}. This is significantly below the correct value, even allowing for some reduction due to anharmonicity.

The best 4-parameter function we found was $F_4(\lambda)$ with a cubic correction term ($p = 3$). This gave an SSR about half that for $f_4(\lambda)$, and also gave a b ratio closer to the predicted value. The addition of another term with $q = 4$ (eq 7) dropped SSR another factor of 10 and gave a b ratio in agreement with predictions. This SSR was a factor of ~3 smaller than that achieved using the 5-parameter $f_5(\lambda)$. The f_4 and f_5 functions also gave better convergence behavior in the decomposition fitting. However, as already noted, they did sometimes yield slightly negative regions in the wings of the component bands (especially for the 5-parameter version).

The computed spectra all display a red shift with increasing T, for both constant and R-dependent transition moment functions. The shift is partly due to the shift in the rotational populations to higher J'' at higher T, an effect that cannot be accommodated in the simple models behind eqs 9 because they do not consider rotation. However, there is also a red shift when the computations are done for fixed J'', as a consequence of the redistribution of the vibrational populations to higher energy in the anharmonic potential wells. This means a move to larger R, where the upper and lower potentials are closer together.

Decomposition Fitting of the Spectrum of Gaseous Br_2. We return to the fitting of the spectrum of Figure 4, except that now we include the previously neglected A ← X transition and we fit simultaneously spectra recorded at 23 °C and 50 °C. Initial tests showed little sensitivity to the vibrational frequency, so this parameter was held at the gas-phase value. Several estimates for the A ← X band are compared with experiment and theory in Figure 7. The curve obtained from log-normal fitting resembles one obtained similarly by Maric et al.[29] and gives the best agreement of the three illustrated cases. However, it greatly exceeds the experimental values from ref 18 and is much too narrow for a realistic A potential. When the C ← X and B ← X bands were represented by the 4-parameter $f_4(\lambda)$, the quality of the fit improved significantly, but the A ← X peak increased its amplitude to >30. In the Gaussian fitting, fixing the location parameter c at the theory-based value also gave a much-too-strong A ← X component. Finally, the three fitted estimates are not remotely consistent in view of their statistical error bands.[61] In short, decomposition fitting has not succeeded in locating the A ← X band of Br_2. In further fitting, this band was fixed at log-normal, using the parameters, $a = 10.0$, $b = 67.17$, and $c = 525.66$ nm, as obtained from the theory curve, scaled to best match the experimental points from ref 18. (Inclusion of the data from ref 24 increases the scale factor by <2%.)

Given the weakness of the A ← X band, it is not surprising that decomposition fitting fails to pin it down. It should also come as no great surprise that in fits in which A ← X is varying as much as discussed above, the other two bands also fail to settle on consensus estimates. So what happens if the A ← X band is fixed at the calculated curve? This is essentially just a repeat of the test of Figure 4, but with A ← X now subtracted. Figure 8 shows that decomposition fitting still fails to yield correct results for the two main component bands, unless the experimental points for B ← X are incorporated in the analysis. When this is done, the component bands also become relatively insensitive to the choice of functional form for their representation. The results from such a fit, as shown by the dashed curves in Figures 3 and 8, are our best estimates of the component bands in the gas-phase spectrum.

I_2 in Solution. Considerable trial-and-error LS fitting was carried out for I_2 in solution, on three separate data sets for heptane and two for CCl_4. The one clear result from these calculations was the characterization of the A ← X band of I_2 in solution (Figure 9). To a good approximation this band in heptane can be obtained by shifting the gas-phase band ~5 nm to the blue (to 673 ± 2 nm) and increasing its intensity by 1 L mol^{-1} cm^{-1} (which is within the error of the gas-phase estimate[21]). All of the fits showed statistically significant red shifts with increasing T, but of varying magnitude. A typical

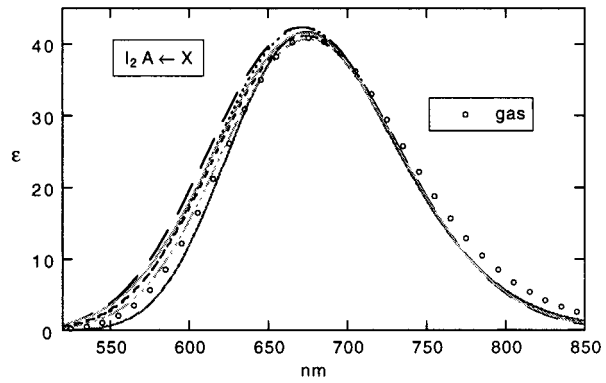

Figure 9. Estimates of the A ← X spectrum of I_2 in *n*-heptane at 23 °C from decomposition fitting of a single data set including spectra at four temperatures. The curve which is lowest in the short-wavelength region was obtained fitting all three components to $f_{GS}(\nu)$, while that which is highest came from a fit in which all bands were represented by $F_4(\lambda)$ (eq 7).

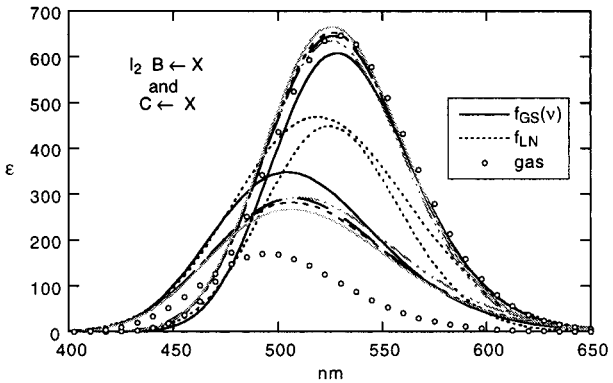

Figure 10. Estimates of the B ← X and C ← X components of I_2 in *n*-heptane at 23 °C from decomposition fitting of the same data as in Figure 9. The unlabeled curves represent statistically comparable results from fits employing different 4-parameter component functions. The log-normal and Gaussian fits (curves identified) gave SSRs higher by factors of 1.3 and 2.8, respectively, than the minimal SSR for this data set.

value was 1.0 nm from 16 °C to 50 °C. Similar results were obtained for all of the data sets.

The same fits of the same data set yielded the estimates of the two stronger components illustrated in Figure 10. The lower-variance 4-parameter fits have roughly converged on a resolution that makes the B ← X band agree approximately with its gas-phase counterpart, thereby attributing essentially all of the increased absorption in solution to a doubling of the intensity of the C ← X band. This band is also significantly red-shifted from its gas-phase location. Fits of the other heptane data sets agreed qualitatively but showed considerable scatter (typically ±50 L mol^{-1} cm^{-1} for each component). In addition, some fits converged on solutions of only slightly higher variance that made the shorter wavelength peak far stronger than the longer, effectively reversing the relationship indicated in Figure 10.

Those fits that converged on components resembling the "consensus" results illustrated in Figure 10 also exhibited an interesting *T* dependence in the peak shifts: The B ← X band showed a small red shift of <1 nm from 16 °C to 50 °C (comparable to that for A ← X), while the red shift for C ← X was about three times greater. These shifts were also much better defined statistically than were those for A ← X.

Results for CCl_4 as solvent were similar to those for heptane but still differed by statistically significant amounts, as would be expected from the differences shown in Figure 5. The main differences were as follows. (1) The A ← X peak is weaker by 10% and is shifted 5 nm further to the blue. (2) The two stronger peaks are blue shifted by slightly more, and they exhibit a stronger *T* dependence in their locations, amounting to >3 nm for C ← X. (3) The total absorption in the main peak tends to be distributed more strongly in favor of B ← X. However, as for I_2 in heptane, the latter two trends must be considered more tenuous in view of the range of results obtainable from different fit models.

TABLE 1: Component Analysis of the Visible Absorption Spectrum of I_2 in *n*-Heptane at 23 °C[a]

parameter[b]	C ← X	B ← X	A ← X
a (L mol^{-1} cm^{-1})	291 (10)	645 (10)	42.32 (8)
b	77.9 (6)	123.0 (5)	63.4 (4)
c (nm)	507.4 (5)	526.40 (13)	670.88 (25)
d (nm^{-3})	4.4 (3) × 10^{-7}	2.27 (12) × 10^{-7}	−5.9 (4) × 10^{-8}
$\Delta\lambda_{16}$ (nm)[c]	−0.40 (3)	−0.11 (2)	−0.3 (1)
$\Delta\lambda_{40}$ (nm)[c]	0.84 (4)	0.25 (2)	0.6 (1)
$\Delta\lambda_{50}$ (nm)[c]	1.36 (6)	0.31 (3)	0.4 (1)
fractional absorption[d]	0.33	0.60	0.069

[a] Wavelength ordering of components assumed to be the same as in the gas phase. [b] As defined for $F_4(\lambda)$, with $p = 3$ (eq 7); 1-σ errors in parentheses, in terms of final digits. [c] Wavelength shift of peak at indicated T (°C, subscript) relative to position in 23 °C spectrum. [d] $\int \epsilon\, d\lambda$ for component, divided by total for all three.

TABLE 2: Absorption Component Analysis for I_2 in CCl_4 at 23 °C[a]

parameter[b]	C ← X	B ← X	A ← X
a (L mol^{-1} cm^{-1})	111 (4)	508 (10)	52.8 (3.5)
b	14.15 (40)	64.2 (1.2)	122 (15)
c (nm)	503.60 (25)	521.17 (13)	664.66 (39)
d (nm)	281 (2)	137 (4)	−251 (61)
ϵ_0 (λ_0)[c]	253 (499.3)	689 (520.4)	38.3 (666.1)
$\Delta\lambda_{16}$ (nm)	−0.62 (2)	−0.27 (1)	−0.9 (1)
$\Delta\lambda_{40}$ (nm)	1.79 (4)	0.58 (1)	−0.6 (1)
$\Delta\lambda_{50}$ (nm)	2.79 (6)	0.90 (13)	0.06 (16)
fractional absorption	0.29	0.65	0.062

[a] All quantities as defined in Table 1 unless otherwise indicated. [b] As defined for $f_4(\lambda)$ (eq 4); 1-σ errors in parentheses, in terms of final digits. [c] Peak amplitude (L mol^{-1} cm^{-1}) and wavelength (nm).

The results for both solvents agree with those of Geilhaupt and Dorfmüller[34] in attributing most of the intensity gain in solution to the C ← X transition. However, these authors found this band to be stronger in CCl_4 than in heptane, opposite to indications from our analysis. If we consider just results obtained fitting to the ν-scaled Gaussian, $f_{GS}(\nu)$ (as did Geilhaupt and Dorfmüller), we do reproduce their trend but find C ← X to be even stronger than they did, exceeding 40% of total absorption for I_2 in CCl_4. (The SSR for these fits was a factor of 2 larger than for the "best" results discussed above.)

The results from representative low-variance fits to 4-parameter band functions are summarized in Table 1 for I_2 in heptane and Table 2 for I_2 in CCl_4.

Br_2 in Solution. For Br_2 in CCl_4, extensive analysis of our best data set yielded the same kind of ambiguities as found in the gas-phase decomposition analysis, so the other solution data sets were not subjected to detailed fitting. In part the problem is the A ← X band, which, though comparable in its relative contribution to the total absorption in I_2 and Br_2, is completely buried under the main peak in Br_2. This might seem to be offset by the better resolution of the two main transitions, but the fitting has failed to confirm this hope.

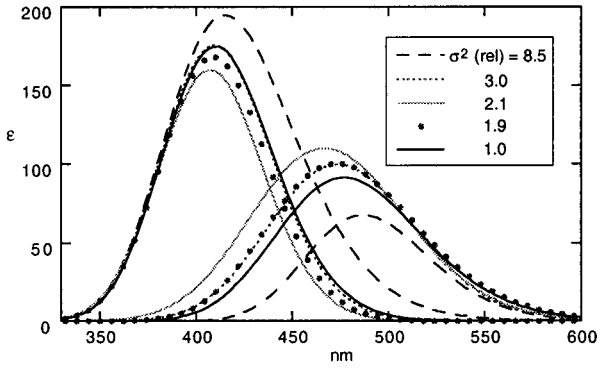

Figure 11. Estimates of the $B \leftarrow X$ and $C \leftarrow X$ components of Br_2 in CCl_4 at 23 °C from decomposition fitting. The results in the label box were obtained by fitting to (from top to bottom): $f_{GS}(\nu)$, $f_{LN}(\lambda)$, $f_4(\lambda)$ ($d = 0$ for $A \leftarrow X$), $F_4(\lambda)$ ($p = 3$, $d = 0$ for $A \leftarrow X$), and $F_4(\lambda)$ ($p = 3$). In all cases the amplitude of the $A \leftarrow X$ band was held at 10.0 L mol^{-1} cm^{-1}, as described in text.

Some results of our attempts at decomposition are illustrated in Figure 11. In all such fitting, the A ← X band was included with its location parameter free but its amplitude fixed at the gas-phase value (10.0). (For the 4- and 5-parameter LN forms of eqs 4 and 5, this also meant setting $d = 0$ for this band.) Even this was not always sufficient to restrain this component. In the fit of lowest SSR in Figure 11, the A ← X band moved to a short wavelength and spread out, becoming, in effect, a broad, shaped background. Excepting the Gaussian fit, which is clearly of lower statistical quality than the others, these results suggest that most of the gain in intensity in solution occurs in the B ← X transition. This seems contrary to naive anticipation from the comparison of gas-phase and solution spectra in Figure 3. And, recalling the lesson of Figure 4, we are reluctant to draw this conclusion.

Refractive Index Corrections. It is common practice in comparing band strengths in solution with those in gas phase to "correct" the solution values for the medium's refraction. For example, IR bands are often compared using the Polo-Wilson equation,[63−65] which is based on the notion that the transition strength is independent of medium. For a band that spans a range of wavelengths, the average transition strength μ^2 is best estimated from $\int \epsilon \, d \ln \nu$ ($= \int \epsilon \, d \ln \lambda$),[54] giving the following version of the Polo-Wilson equation:

$$\frac{\int \epsilon_{sln} \, d \ln \lambda}{\int \epsilon_g \, d \ln \lambda} = \frac{1}{n_r}\left(\frac{n_r^2 + 2}{3}\right)^2 \frac{\mu_{sln}^2}{\mu_g^2} \qquad (10)$$

where n_r is the refractive index. This and other forms have been applied to electronic spectra as well.[35,66] If μ^2 is the same in solution and in vacuo, the integrated absorption spectra in solution and gas phase should display the indicated dependence on n_r. But experimental support for this notion has not always been convincing,[35,64] and it is not in the present case. For example, while it is true that eq 10 predicts the solution spectra to be stronger, the predicted increase is 30% rather than 20%. Clearly eq 10 worsens the agreement for A ← X in I_2, where the uncorrected spectra already agree within 5%. Further, the T dependence of n_r for our solvents leads to a 1% decrease in the correction factor on going from 16° to 50 °C. However, for our solution spectra, the integral in eq 10 is constant within 0.1% for most analyzed data sets. It appears that the simple models behind eq 10 and other n_r-based corrections[66] are of little use in explaining the gas vs solution differences explored in the present work.

Conclusion

We have recorded precise absorption spectra for I_2 dissolved in *n*-heptane and in CCl_4, at temperatures from 16 °C to 50 °C. Through simultaneous least-squares fitting of these spectra to models that specifically take this T dependence into account, we have extracted estimates of the contributions of the three electronic transitions responsible for the visible-near-IR absorption. The results confirm earlier indications that the weakest band, A ← X, is very nearly the same in intensity and shape as in the gas phase, though blue shifted in solution. They also suggest that most of the ∼20% increase in total absorption in these solvents occurs in the C ← X transition, with the strongest band, B ← X, being again similar to its gas-phase counterpart in shape and intensity. However, the assessment of these two transitions is much more tenuous than that of A ← X and will require further substantiation.

Similar efforts for Br_2 dissolved in CCl_4 have yielded inconclusive results, with at most the suggestion that B ← X, which is weaker than C ← X in Br_2, accounts for more of the absorption gain in solution. With its higher vibrational frequency, Br_2 shows less sensitivity than I_2 to temperature changes accessible to us in these experiments, which were restricted to the smaller range 16° − 40 °C.

In the course of these studies we have conducted a number of tests of the assumptions of band decomposition analysis. Specifically we have shown the following. (1) The 3-parameter Gaussian and log-normal functions widely used to represent component bands do not have enough flexibility to match the statistical quality of absorption spectra routinely available from commercial spectrophotometers. (2) When used to decompose an overlapped spectrum, these two forms can yield wildly different components, even though they appear to perform comparably in representing the total spectrum. (3) The observation of lower fit variance is no guarantee that the resulting decomposition is closer to "true." To get around these limitations, we have examined the results from a range of different assumed band functions having at least four adjustable parameters, in quest of a "convergence" on components that are independent of the choice of function. In the absence of such an examination of model dependence, the practitioners of band decomposition analysis would be well advised not to "bet the farm" on the validity of their decompositions.

Of course, one reason it is even feasible to attempt a component analysis for spectra like those obtained here for I_2 and Br_2 is the very high quality of data easily obtained in abundance from modern specrophotometers. As was noted earlier, in many applications of component analysis, the components are more a means to an end than a goal in themselves. As a way of compactly representing overlapped spectra in terms of easily used expressions, as for example in atmospheric modeling,[28,29] such analyses may be entirely adequate, as the demands for these applications seldom push the limits of experimental accuracy and precision.

Band decomposition analysis as utilized in this work can be considered a phenomenological method, in that the parameters in the fit model are mostly ad hoc in nature. It is worth asking whether a physical model, in which the parameters are used to describe the potential curves and transition moment functions involved in the spectral transitions, might perform better. Indeed it did in the analysis of T-dependent absorption in gaseous Br_2 carried out by Le Roy, et al.[5] As was noted earlier, that work profited from reliable existing information about the shapes of the bound regions of the potential wells. Some such information is available about I_2 and Br_2 in simple solvents,

including vibrational frequencies and anharmonicities in the ground states.[58,62] So it is worth asking whether such a physical model might also work better for the solution spectra. The answer to that question must remain a topic for future study, as must also the refined analysis of the Br_2 gaseous absorption with proper accounting for the A ← X absorption.

Acknowledgment. We thank Robert Le Roy and Mario Fajardo for fruitful conversations on the topic of this work and for sending us ref 65 prior to its publication. We also thank Dubravko Maric for alerting us to the notation problem for the $^1\Pi$ states and for other helpful suggestions following a critical reading of our manuscript.

Supporting Information Available: Absorption spectra of I_2 in *n*-heptane, I_2 in CCl_4, Br_2(g), and Br_2 in CCl_4 are available in Tables 1S−4S, obtainable free of charge via the Internet at http://pubs.acs.org. The solution spectra are tabulated at four temperatures, the Br_2(g) spectra at two.

References and Notes

(1) Mulliken, R. S. *J. Chem. Phys.* **1971**, *55*, 288.
(2) Huber, K. P.; Herzberg, G. *Constants of Diatomic Molecules*; Van Nostrand Reinhold: New York, 1979.
(3) Coxon, J. A. *J. Mol. Spectrosc.* **1972**, *41*, 566.
(4) Barrow, R. F.; Clark, T. C.; Coxon, J. A.; Yee, K. K. *J. Mol. Spectrosc.* **1974**, *51*, 428.
(5) Le Roy, R. J.; Macdonald, R. G.; Burns, G. *J. Chem. Phys.* **1976**, *65*, 1485.
(6) Clyne, M. A. A.; Heaven, M. C.; Tellinghuisen, J. *J. Chem. Phys.* **1982**, *76*, 5341.
(7) Seery, D. J.; Britton, D. *J. Phys. Chem.* **1964**, *68*, 2263.
(8) Passchier, A. A.; Christian, J. D.; Gregory, N. W. *J. Phys. Chem.* **1967**, *71*, 937.
(9) Busch, G. E.; Mahoney, R. T.; Morse, R. I.; Wilson, K. R. *J. Chem. Phys.* **1969**, *51*, 837.
(10) Oldman, R. J.; Sander, R. K.; Wilson, K. R. *J. Chem. Phys.* **1971**, *54*, 4127.
(11) Tellinghuisen, J. *J. Chem. Phys.* **1973**, *58*, 2821.
(12) Oldman, R. J.; Sander, R. K.; Wilson, K. R. *J. Chem. Phys.* **1975**, *63*, 4252.
(13) Brith, M.; Rowe, M. D.; Schnepp, O.; Stephens, P. J. *Chem. Phys.* **1975**, *9*, 57.
(14) Zaraga, F.; Nogar, N. S.; Moore, C. B. *J. Mol. Spectrosc.* **1976**, *63*, 564.
(15) Williams, P. F.; Fernandez, A.; Rousseau, D. L. *Chem. Phys. Lett.* **1977**, *47*, 150.
(16) Peterson, A. B.; Smith, I. W. M. *Chem. Phys.* **1978**, *30*, 407.
(17) Lindeman, T. G.; Wiesenfeld, J. R. *J. Chem. Phys.* **1979**, *70*, 2882.
(18) Hemenway, C. P.; Lindeman, T. G.; Wiesenfeld, J. R. *J. Chem. Phys.* **1979**, *70*, 3560.
(19) De Vries, M. S.; Van Veen, N. J. A.; Hutchinson, M.; De Vries, A. E. *Chem. Phys.* **1980**, *51*, 159.
(20) Wiesenfeld, J. R.; Young, R. H. *Chem. Phys.* **1981**, *58*, 51.
(21) Tellinghuisen, J. *J. Chem. Phys.* **1982**, *76*, 4736.
(22) Burkholder, J. B.; Bair, E. J. *J. Phys. Chem.* **1983**, *87*, 1859.
(23) Haugen, H. K.; Weitz, E.; Leone, S. R. *J. Chem. Phys.* **1985**, *83*, 3402.
(24) Smedley, J. E.; Haugen, H. K.; Leone, S. R. *J. Chem. Phys.* **1987**, *87*, 2700.
(25) Strempel, J.; Kiefer, W. *Can. J. Chem.* **1991**, *69*, 1732.
(26) Strempel, J.; Kiefer, W. *J. Raman Spectrosc.* **1991**, *22*, 583.
(27) Mashnin, T. S.; Chernyshev, A. V.; Krasnoperov, L. N. *Chem. Phys. Lett.* **1993**, *207*, 105.
(28) Maric, D.; Burrows, J. P.; Meller, R.; Moortgat, G. K. *J. Photochem. Photobiol. A: Chem.* **1993**, *70*, 205.
(29) Maric, D.; Burrows, J. P.; Moortgat, G. K. *J. Photochem. Photobiol. A: Chem.* **1994**, *83*, 179.
(30) Cao, J.; Loock, H.-P.; Qian, C. X. W. *Can. J. Chem.* **1994**, *72*, 758.
(31) Hubinger, S.; Nee, J. B. *J. Photochem. Photobiol. A: Chem.* **1995**, *86*, 1.
(32) Jung, K.-W.; Ahmadi, T. S.; El-Sayed, M. A. *J. Phys. Chem. A* **1997**, *101*, 6562.
(33) Ham, J. *J. Am. Chem. Soc.* **1954**, *76*, 3886.
(34) Geilhaupt, M.; Dorfmüller, Th. *Chem. Phys.* **1983**, *76*, 443.
(35) Sension, R. J.; Strauss, H. L. *J. Chem. Phys.* **1986**, *85*, 3791.
(36) Sension, R. J.; Strauss, H. L. *J. Chem. Phys.* **1988**, *88*, 2289.
(37) Schenk, M.; Kiefer, W. *J. Chem. Phys.* **1996**, *105*, 2177.
(38) Sulzer, P.; Wieland, K. *Helv. Phys. Acta* **1952**, *25*, 653.
(39) Siano, D. B.; Metzler, D. E. *J. Chem. Phys.* **1969**, *51*, 1856.
(40) Maric, D.; Burrows, J. P. *J. Phys. Chem.* **1996**, *100*, 8645.
(41) Maric, D.; Crowley, J. N.; Burrows, J. P. *J. Phys. Chem.* **1997**, *101*, 2561.
(42) Langhals, H. *Spectrochim. Acta, A* **2000**, *56*, 2207.
(43) Tellinghuisen, J. *Appl. Spectrosc.* **2000**, *54*, 1208.
(44) Herzberg, G. *Spectra of Diatomic Molecules*; D. Van Nostrand: New York, 1950.
(45) Clear, R. D.; Wilson, K. R. *J. Mol. Spectrosc.* **1973**, *47*, 39.
(46) Hwang, H. J.; El-Sayed, M. A. *J. Phys. Chem.* **1991**, *95*, 8044.
(47) Tellinghuisen, J. *Appl. Spectrosc.* **2000**, *54*, 431.
(48) Riddick, J. A.; Bunger, W. B.; Sakano, T. K. *Organic Solvents*, 4th ed.; Wiley: New York, 1986.
(49) Sanni, S. A.; Fell, C. J. D.; Hutchison, H. P. *J. Chem. Eng. Data* **1971**, *16*, 424.
(50) Deshpande, D. D.; Bhatgadde, L. G. *Aus. J. Chem.* **1971**, *24*, 1817.
(51) Smith, B. D.; Srivastava, R. *Thermodynamic Data for Pure Compounds*, Elsevier: New York, 1986.
(52) Tellinghuisen, J. *J. Phys. Chem. A* **2000**, *104*, 2834.
(53) Barthel, C. *Bull. Soc. Chim. (France)* **1970**, 1676.
(54) Tellinghuisen, J. *Adv. Chem. Phys.* **1985**, *60*, 299.
(55) Tellinghuisen, J. *J. Chem. Phys.* **1984**, *80*, 5472.
(56) Hwang, E.; Dagdigian, P. J.; Tellinghuisen, J. *J. Mol. Spectrosc.* **1997**, *181*, 297.
(57) Viswanathan, K. S.; Sur, A.; Tellinghuisen, J. *J. Mol. Spectrosc.* **1981**, *86*, 393.
(58) Put, J.; Maes, G.; Huyskens, P.; Zeegershuyskens, T. *Spectrochim. Acta A* **1981**, *37*, 699.
(59) Bevington, P. R. *Data Reduction and Error Analysis for the Physical Sciences*; McGraw-Hill: New York, 1969.
(60) Press, W. H.; Flannery, B. P.; Teukolsky, S. A.; Vetterling, W. T. *Numerical Recipes*; Cambridge University Press: Cambridge, U. K., 1986.
(61) Tellinghuisen, J. *J. Phys. Chem. A* **2001**, *105*, 3917.
(62) Kiefer, W.; Bernstein, H. J. *J. Raman Spectrosc.* **1973**, *1*, 417.
(63) Polo, S. R.; Wilson, M. K. *J. Chem. Phys.* **1955**, *23*, 2376.
(64) Bertie, J. E.; Keefe, C. D. *J. Chem. Phys.* **1994**, *101*, 4610.
(65) Tam, S.; Fajardo, M. E. *Appl. Spectrosc.*, in press.
(66) Strickler, S. J.; Berg, R. A. *J. Chem. Phys.* **1962**, *37*, 814.